Carbon Emission Analysis of Precast Concrete Building Construction: A Study on Component Transportation Phase using Artificial Neural Network

Haining Wang[1], Liang Zhao[2], Hong Zhang[1], Yuchong Qian[1]*, Yiming Xiang[3], Zhixing Luo[4], Zixiao Wang[1],

[1]School of Architecture, Southeast University, Nanjing 210096, P.R. China

[2]School of energy and environment engineering, Hebei University of Engineering, Handan 056038, P.R. China

[3]Bartlett School of Sustainable Construction, University College London, London WC1E 7HB, UK

[4]State Key Laboratory of Green Building, Xi'an University of Architecture and Technology, Xi'an 710055, P.R. China

* Corresponding author: ycqian_seu@126.com (Yuchong Qian)

Abstract

Off-site construction has been widely adopted for its carbon reduction potential. However, the emissions from its transportation stage are not fully explored. Given the rising prominence of Battery Electric Vehicles (BEVs), this study explores their potential carbon reduction benefits during the transportation of prefabricated components by comparing emissions from Fossil Vehicles (FVs) and BEVs. An Artificial-Neural-Network-based emission model is developed to estimate the carbon emissions of both vehicle types. Specifically, the model collects the real-time carbon emission dynamics across varying external conditions, encompassing diverse transportation constraints, vehicle operational statuses, and road conditions. By employing a supervised learning framework, the transportation carbon emission coefficient of prefabricated components is determined. Comparative analysis reveals that BEVs consistently outperforms FVs, achieving a peak reduction rate of 47.76%. The negative correlation between the reduction rate of BEVs and factors like average speed and load rate underscores BEVs' advantage in urban transportation scenarios, where these factors tend to be low. Hence, the integration of BEVs in the transportation of prefabricated components is advocated. This study provides robust carbon emissions coefficients for BEVs in the transportation of prefabricated components, filling the gap in current estimation methods. These coefficients present a valuable tool for researchers, aiding in the accurate estimation of transportation carbon emissions and fostering the conceptualization of innovative carbon reduction tactics through BEV adoption.

Keywords: Carbon Emission; Prefabricated Component Transportation; Battery Electric Vehicle; Artificial Neural Network; Precast Concrete Building

Nomenclature

Abbreviations

CE	carbon emission
CEF	carbon emission factor
PCB	prefabricated concrete building
PC	prefabricated component
PCT	prefabricated component transportation
FV	fossil vehicle
BEV	battery electric vehicle
ANN	artificial neural network

Variables

LR	load rate of single vehicle
AS	average speed
T	atmosphere temperature
TOV	type of vehicle
CTF	component transportation factor
F	factor of carbon emission
CE	carbon emission of component transportation
b	number of buildings for specific project
k	number of vehicles required to transport components for specific building
p	number of components for specific vehicle
E	energy consumption
d	distance of component transportation
M	the weight of components
θ	energy consumption efficiency

Subscript

ep	entire project
sb	single building
sv	single vehicle
ct	component transportation
FV	fossil vehicle
f	fossil fuel
BEV	battery electric vehicle
e	electric

1. Introduction

The Architecture, Engineering, and Construction (AEC) industry has a significant impact on global carbon emissions, contributing to 37% of the total carbon emissions (CE) [1]. China, as the largest emitter of carbon emissions, and has set a goal to peak its emissions by around 2030 [2]. To achieve this target, it is crucial to implement effective carbon control measures within the AEC sector, especially the building sectors inside [3]. The AEC industry is responsible for a substantial portion of the country's carbon emissions in China, accounting for approximately 27.9-34.3% from 1995 to 2010 [4].

The carbon footprint of a building's entire lifecycle can be classified into two categories: embodied carbon and operation carbon [5]. In the context of China's total CE, which reached 13.9 billion tCO_2 in 2020, the building sector contributed 1.5 billion tCO_2 in embodied carbon and 2.2 billion tCO2 in operation carbon [6]. Embodied carbon emissions occur during various stages such as raw material and component production, transportation, construction, maintenance, and demolition. On the other hand, operation carbon is generated by the energy used for activities such as air conditioning, ventilation, heating, lighting, and operating building equipment [7, 8]. Although embodied carbon only accounts for 8%-20% of a building's total carbon emissions over its lifespan [9-12], it has s relatively shorter emission duration compared to the operation carbon, which can span several decades [13]. However, embodied carbon exhibits a higher intensity of carbon emissions per unit of time. Therefore, it plays a critical role in the overall efforts to mitigate carbon emissions.

The use of Prefabricated Concrete Building (PCB) technology offers a compelling alternative to the traditional on-site construction approach by shifting a significant portion of construction work from the actual construction site to controlled factory environments. This not only improves construction efficiency, but also reduces labor demands [14] and minimizes construction waste generation, making it a promising sustainable construction solution [15]. Moreover, PCB technology has gained increasing recognition, particularly in response to the anticipated labor shortage resulting from an aging population in some developing countries [16]. Consequently, it has garnered significant attention and support, with some regions even implementing policies to ensure a certain proportion of newly constructed buildings adopting PCB technology, particularly for large-scale residential projects [17]. Notably, PCB exhibits lower carbon emissions compared to conventional cast-in-site construction methods in some real-world engineering applications [18].

By adopting PCB technology, Hao et al. [19] achieved a notable 15% reduction in embodied CE. However, it is crucial to examine the specifics, as the current situation reveals that Prefabricated

Component Transportation (PCT) can result in an increase in CE. For instance, while this construction method reduces building waste, Wong and Tang [20] argued that it may actually result in higher CE during transportation and manufacturing processes. Dong et al. [21] asserted that, when compared to conventional construction method, the PCT process contributes to an alarming 88% increase in transportation-related carbon emissions. In some real-world projects, Mao et al. [22] found that PCT for prefabricated panels offset approximately 15.3% of the carbon emission reduction achieved during the entire embodied carbon phase. Additionally, Xiang et al. [23] found that PCB can reduce embodied carbon by 3% through waste reduction, whereas PCT resulted in a concerning 4% increase in CE. It is evident that, at the current technical level, the PCT phase is crucial for controlling carbon emissions and improving the carbon reduction potential of PCB.

The materialization phase of PCB includes five distinct phases: material production, material transportation, component production, component transportation, and construction [24]. In contrast, the cast-on-site construction simplies this process, including only three phases: material production, material transportation, and construction. The transportation aspect of PCB includes two separate phases: material transportation and component transportation. In some PCB projects, these two phases can account for up to 10% of CE [25]. The aforementioned outcomes are tied to the core components of PCB, known as Prefabricated Components (PCs). PCs are integrated building products that combine various construction materials, allowing for easier materialization work and streamlining on-site construction processes. However, it is important to consider that PCs are indivisible products [26], characterized by larger dimensions and higher storage demands, compared to scattered building materials. These factors pose size limitations during highway transportation and time constraints during on-site construction, which greatly impact the efficiency of PCT. Consequently, the limited efficiency of PCT results in energy wastage and increased CE associated with the transportation process [25].

Thus, it is necessary to establish a CE calculation system for PCB that focuses on its components rather than materials used. This system should also include Carbon Emission Factor (CEF) associated with PCB. The calculation of CEF should take into account several factors, such as low speed, limited range, frequent stops, extended idle times, and low carrying capacity. Low speed can result in reduced transmission efficiency, leading to higher energy consumption. Limited range means that a significant portion of energy is consumed during engine startup, which is less efficient compared to long range transportation. Frequent stops cause more idle times, representing extremely low energy efficiency. Lastly, low carrying capacity means that more energy is used to move the vehicle's weight itself, rather than for its intended components. Those complex situations covering several operating stages of vehicle [27] are difficult to simulate in sophisticated laboratories, but can effectively demonstrate the real performance of PCT. By making these efforts, the potential for reducing embodied carbon in PCB can be increased.

Energy is consumed to power vehicles and transport PCs within a specific area, which directly contributes to the generation of CE. The prevalent method for PCT relies heavily on road transport, mainly utilizing Fossil Vehicles (FVs) that run on diesel or gasoline. It is essential to note that FVs have considerably higher CEF compared to alternative transportation modes such as railways or waterways. Therefore, to effectively address the issue of high emissions in PCT, it is crucial to address the issue at its core by selecting low-carbon energy sources as a fundamental solution.

In recent years, some developing countries have been consistently providing subsidies for new energy vehicles, particularly BEVs [28]. This has led to the widespread adoption of BEVs, starting from passenger cars and gradually expanding to cargo transportation. One significant advantage of BEVs is that they do not consume fossil fuels during operation, resulting in zero direct CE [29]. BEVs utilize electric motors and battery packs, instead of internal combustion engines and fuel tanks found in traditional vehicles. Additionally, BEVs yield lower carbon emissions during their operational lifespan. Zhou et al. [30] asserted that the electric motors in BEVs have a much higher energy conversion efficiency compared to internal combustion engines powered by diesel or gasoline. Moreover, the use of BEVs benefits from the carbon advantages of electricity supply and distribution systems, further reducing their carbon footprint [31]. Overall, these characteristics make BEVs a more environmentally-friendly choice with significantly lower carbon emissions compared to conventional vehicles [27,28].

Despite current limitations of BEV, the specific requirements and characteristics of prefabricated construction help mitigate any potential adverse effects. Firstly, the shorter driving range of BEVs does not have a significant impact in this scenario. It is true that BEVs currently have limitations in terms of their driving range compared to traditional fossil vehicles FVs [29,30]. However, in prefabricated building projects, where there are limitations on the economic transportation radius [31], most components are sourced from local factories within the same city. Moreover, BEVs have lower energy consumption when idle compared to FVs [32, 33]. Since prefabricated construction sites are often located in densely populated urban areas, there are frequent stops and longer waiting times at traffic lights. This means that the limitations of BEV driving range are offset by their improved energy efficiency during stop-and-go traffic conditions commonly encountered in urban settings.

In summary, the distinctive features of BEVs effectively meet the sustainability requirements in the process of PCB construction, particularly in the case of PCT, which significantly enhances the potential for reducing carbon emission. However, existing research on BEVs in transportation mainly focuses on the vehicles and improving transportation routes for large quantities of materials [34-37]. Unfortunately, there is a significant lack of research focused on prefabricated components (PCs) and the associated carbon emissions in the PCT process.

This gap becomes more apparent when considering China's current carbon emission calculation standards [38], which solely account for transportation modes for bulk and scattered materials, offering different emission factors for various levels of FVs, railways, and water transportation. However, these standards overlook the importance of BEVs used in transportation and do not provide specific emission factors for their use. Moreover, these standards do not encompass the unique characteristics of PCs, do not establish targeted calculation methods, models, and factors that accurately reflect the true carbon emission characteristics of PCT. As a result, they fall short in facilitating the necessary optimizations in architectural design, component design, and construction organization.

This research specifically focuses on studying CE in relation to precast concrete (PC) in the construction industry. The main objective is to develop a calculation method that accurately estimates CE during the design phase, with PCs as the primary unit of analysis. To achieve this, a series of comprehensive road transportation experiments were conducted to simulate real-world PCT scenarios. These experiments involved both FVs and BEVs, gathering firsthand data. The collected data was meticulously analyzed to identify and quantify the influence of various external factors on CE. Additionally, advanced machine learning techniques were employed to perform regression analysis to create a robust carbon emission calculation model, along with the corresponding CEF (as shown in Figure 1).

The research outcomes have significant implications for both industry policy-making and individual companies with the construction industry. At the macro level, the study quantitatively assess the potential reduction in carbon emission that can be achieved by the application of BEVs. This assessment provides valuable information for industry regulatory bodies, empowering policymakers to make well-informed decisions regarding carbon reduction strategies. On the micro level, the research identifies and analyzes the factors that limit carbon emission during the PCT process, providing computational tools for optimizing CE in the design of sustainable prefabricated buildings.

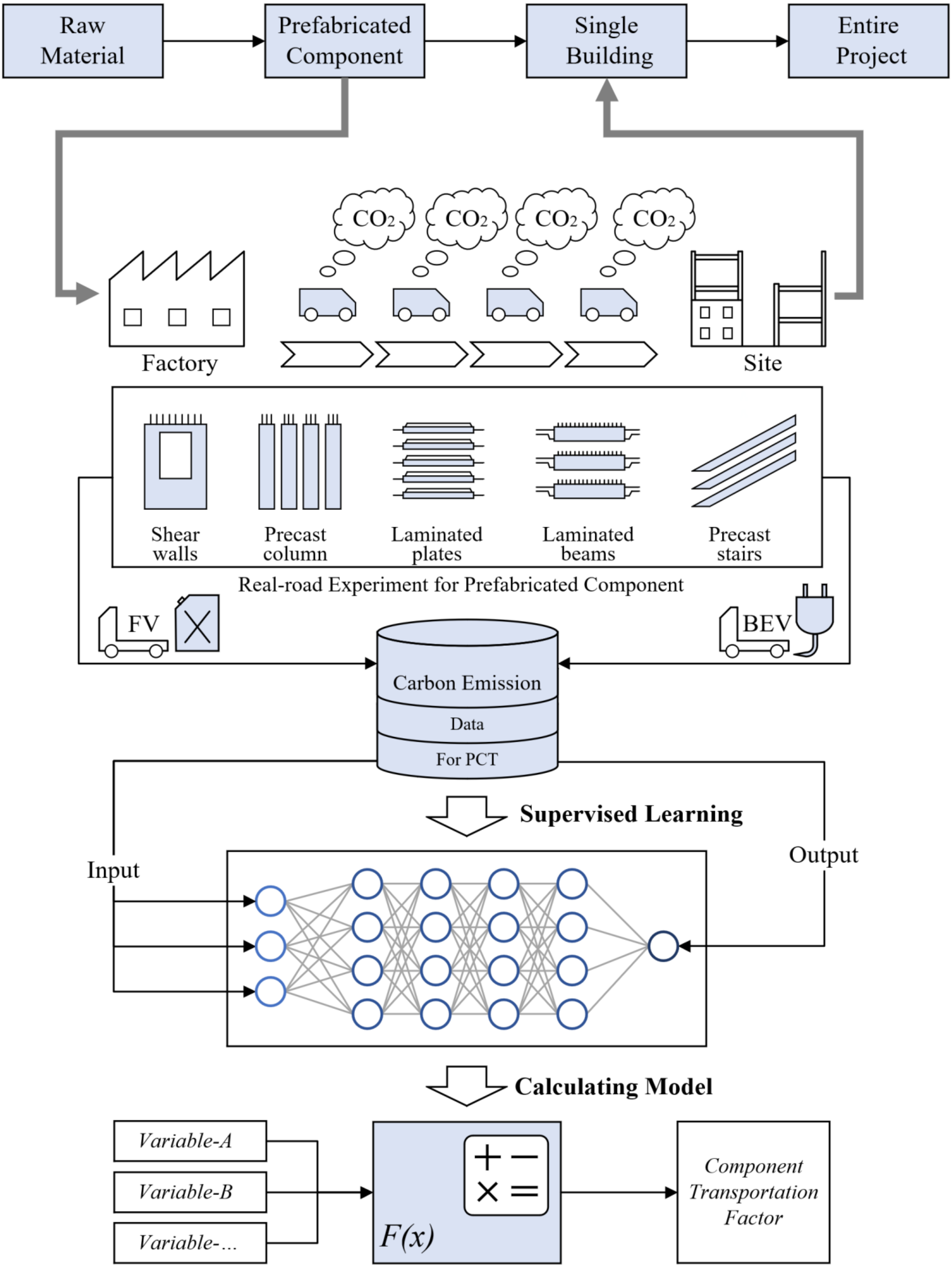

Figure 1 Research framework

2. Methodology

The methodology employed in this study is a bottom-up, process-based life cycle assessment approach, focusing on a micro-level analysis of specific PCs. By tracking their transportation processes and conducting a thorough analysis, this method utilizes comprehensive building carbon emission factors to achieve a reasonably accurate estimation of carbon emissions.

2.1 System boundary

This study focuses on the carbon emissions associated with the transportation of prefabricated components using FV and BEV. Therefore, our investigation is limited to the calculation and estimation of carbon emissions typically observed during this phase. The emissions related to the use of lifting tools during the lifting process of components are not considered. For the carbon emissions resulting from the use of lifting tools at the factory and on-site are accounted for in the Component Production Phase and Construction Phase, respectively.

Throughout the PCT process, we assume, no unforeseen circumstances occur, such as vehicle engine breakdown, battery package disorder, or unusual weather conditions like rain, snow, or typhoon. However, considering that a significant number of prefabricated buildings are located in urban areas and that component transportation occurs throughout the day, the potential occurrence of traffic congestion is taken into account. This includes instances of waiting at red lights and idling during traffic jams, which result in increased consumption of fossil fuels and electricity due to lower speeds.

2.2 Data collection

The Kyoto Protocol identifies six major greenhouse gases, namely carbon dioxide (CO_2), methane (CH_4), nitrous oxide (N_2O), hydrofluorocarbons (HFCs), perfluorocarbons (PFCs), and sulfur hexafluoride (SF_6) [39]. In this study, the term "carbon dioxide equivalent" (CO_2e) is used to represent the overall environmental quality of these six gases. Since the focus of this research is on the direct and indirect carbon emissions caused by the PCT process, and the emissions of HFCs, PFCs, and SF_6 in this process are negligible, the CO_2e considered in this study only includes the emissions of CO_2, CH_4, and N_2O resulting from the consumption of fossil fuels and electricity in the preparation, transportation, and work processes of the PCT process. So, the fuel and electricity consumed will be collected by digital device of the vehicle, as well as some other data which can descript the objective situation.

2.3 Model for calculating CE

For Project PCB, the CE during the PCT process is composed of the cumulative CE from the PCT processes of all individual buildings within the project. It should be noted that the specific CE for a particular building's PCT process is determined by the transportation of specific components in different rounds. The choice of vehicle types for each round can significantly differ due to factors such as the arrangement of components, various component manufacturers, and traffic control measures during site access. Consequently, the CE needs to be separately calculated and then aggregated (as indicated in Formula 01).

$$\boldsymbol{CE_{ep}} = \sum_{i=1}^{b} \boldsymbol{CE_{sb}^{i}} = \sum_{i=1}^{b}\left(\sum_{j=1}^{k} \boldsymbol{CE_{sv}^{j}}\right) \qquad \boldsymbol{Formula\ 01}$$

Where, $\boldsymbol{CE_{ep}}$***is the carbon emissions during the component transportation phase of a specific project, measured in kg-CO₂e;***

$\boldsymbol{b}$***is the total number of individual buildings within the project, measured in units of buildings;***

$\boldsymbol{CE_{sb}^{i}}$***is the carbon emissions during the component transportation phase of the ith individual building, measured in kg-CO₂e;***

$\boldsymbol{k}$***is the number of vehicles required for the component transportation of the individual building, measured in units of vehicles;***

$\boldsymbol{CE_{sv}^{j}}$ ***is the direct and indirect carbon emissions generated by the jth vehicle during the component transportation process, measured in kg-CO₂e.***

For a specific vehicle during the PCT process, the quantity of CE is determined by the direct and indirect emissions from the consumed energy. When using a FV, it is determined by the quantity of fossil fuels consumed and the CEF associated with those fuels. When using a BEV, it is determined by the amount of electricity consumed and the CEF for electricity. (as shown in Formula 02).

It is important to note that the CEF for fossil fuels and electricity is a fixed value. Therefore, the variation in CE is determined by the amount of energy consumed. However, this value cannot be accurately obtained before the PCT activity takes place, which does not align with the principle of pre-calculating carbon emissions. On the other hand, the energy consumption per 100 kilometers for vehicles is a more common performance indicator, which can be estimated based on the objective conditions under which the vehicles operate.

$$CE_{sv} = E \times F = 100 \times \theta \times d \times F \qquad \textit{Formula } 02$$

Where, CE_{sv} is the direct and indirect carbon emissions generated by a specific vehicle during the component transportation process, measured in kg-CO_2e;

E is the energy consumption during the PCT process. When using a FV, it is measured in L. When using a BEV, it is measured in kWh;

F is the carbon emission factor of the consumed energy. When using a FV, it is measured in kg-CO_2e/L. When using a BEV, it is measured in kg-CO_2e/kWh;

θ is the energy consumption per 100 kilometers traveled by the vehicle. When using a FV, it is measured in L/100km. When using a BEV, it is measured in kWh/100km;

d is the distance traveled during the PCT process, measured in km.

According to the specifications of the GB/T 2589-2008 standard, the calculation of CE during the PCT process can be expressed using Formula 03. This formula establishes a direct proportionality between CE and two factors: the weight of the components $\sum_{i=1}^{p} M^i$ and the transportation distance d. These two factors can be obtained prior to the occurrence of PCT activities. The transportation distance is determined by the location between the component factory and the project site, while the component weight is derived from the PC transportation plan. Therefore, the crucial aspect of carbon emissions assessment in the PCT process lies in obtaining accurate CEF, which represent the numerical values of the parameters (F_{ct}) and accurately reflect the current situation.

$$CE_{sv} = F_{ct} \times d \times \sum_{i=1}^{p} M^i \qquad \textit{Formula } 03$$

Where, CE_{sv} is the direct and indirect carbon emissions generated by a specific vehicle during the component transportation process, measured in kg-CO_2e;

F_{ct} is the CEF for the PCT phase, measured in kg-CO_2e/(t·km);

d is the transportation distance during the PCT process, measured in km;

p is the quantity of prefabricated components carried by the vehicle, measured in units of pieces;

M^i is the weight of the ith prefabricated component, measured in tonnes.

By combining Formula 02 and Formula 03, the calculation formula for the CEF during the component transportation is derived, using FV, denoted as Formula 04. Similarly, for the component transportation using BEV, Formula 05 is obtained. These formulas reflect the experimental logic of this study, providing the CEF values under different conditions.

In the experimental measurement process, θ_f and θ_e represent the common variables used to measure the energy efficiency of the transportation vehicles, indicating the amount of energy consumed per 100 kilometers, which can be obtained from the vehicle's onboard computer during the experiment. F_f and F_e represent the corresponding energy carbon emission factors, which are assumed to be constant under certain conditions. $\sum_{i=1}^{p} M^i$ represents the total mass of the components currently being transported by the vehicle. While this value is known for the current experiment, it can vary significantly due to factors such as construction organization plans, component transportation requirements, cargo space limitations, and road transportation requirements.

$$\boldsymbol{F_{ct-FV} = 100 \times \theta_f \times F_f \Big/ \sum_{i=1}^{p} M^i} \qquad \textbf{\textit{Formula} 04}$$

$$\boldsymbol{F_{ct-BEV} = 100 \times \theta_e \times F_e \Big/ \sum_{i=1}^{p} M^i} \qquad \textbf{\textit{Formula} 05}$$

Where, F_{ct-FV} is the CEF during component transportation using FV, measured in kg-$CO_2e/(t\cdot km)$;

θ_f is the energy use efficiency of FV during component transportation, measured in L/100km;

F_f is the CEF for the fossil fuel consumed by FV, measured in kg-CO_2e/L;

p is the quantity of prefabricated components currently carried by the vehicle, measured in units of pieces;

M^i is the weight of the ith prefabricated component, measured in tonnes;

F_{ct-BEV} is the CEF during component transportation using BEV, measured in kg-$CO_2e/(t\cdot km)$;

θ_e is the energy use efficiency of BEV during component transportation, measured in kWh/100km;

F_e is the CEF for the electricity consumed by BEV, measured in kg-CO_2e/kWh.

2.4 Model training

2.4.1 Definition of prediction model

The prediction of CE during the PCT process involves the estimation of CEF. By utilizing these factors, it becomes feasible to evaluate the future total CE based on identifiable influencing factors during the design phase. This assessment provides insights into the feasibility of current building designs and construction organization plans in terms of managing carbon emissions.

Obtaining the CEF requires a significant amount of real CE data from the PCT process in existing PCB projects. These data are analyzed and statistically examined using relevant regression algorithms. Through fitting analysis, the contributions of different influencing factors to CEF are determined, aiming to meet certain fitting criteria. This process enables the derivation of predictive models that can estimate CEF based on the identified factors.

2.4.2 Data preprocessing

To accelerate the optimization process and avoid numerical errors caused by differences in dimensional units and magnitudes among various indicators, this study normalizes the input factors of the model. Normalization transforms the numerical values of the factors to the range (0, 1]. The commonly used linear function normalization is employed in this study. Additionally, to prevent the issue of vanishing gradients during training due to any factor having a value of zero, a small constant value of σ = 0.000001 is used. The normalization formula is shown as Formula 06:

$$\boldsymbol{X_{norm} = \frac{X - X_{min}}{X_{max} - X_{min}} + \sigma} \qquad \textbf{\textit{Formula}}\ \mathbf{06}$$

Where, $\boldsymbol{X_{norm}}$***is the normalized value of the indicator after normalization;***

$\boldsymbol{X}$ ***is the original value of the factor;***

$\boldsymbol{X_{max}}$ ***is the maximum value of the factor;***

$\boldsymbol{X_{min}}$ ***is the minimum value of the factor;***

$\boldsymbol{\sigma}$ ***is the compensation intercept term.***

2.4.3 Index for evaluation of prediction model

In this study, the optimisation and selection of the predictive model are defined based on the following three criteria.

(1). Mean squared error

The Mean Squared Error (MSE) measures the average of the squared differences between the predicted values and the corresponding actual values. A lower MSE indicates a better fit of the computational model, with reduced dispersion in the predicted data. In this study, MSE is employed as the loss function for various machine learning algorithms, and the optimization direction of the fitting model is determined by minimizing this metric. The calculation formula for MSE is shown as Formula 07:

$$\boldsymbol{MSE = \frac{1}{n} \times \sum_{i=1}^{n} (y_i - \hat{y}_i)} \qquad \textbf{\textit{Formula} 07}$$

Where, MSE is Mean squared error;

n is the number of data points;

y_i is the actual value of the ith data point;

$\hat{y}_i$ is the predicted value of the ith data point.

(2). Coefficient of determination

The coefficient of determination, denoted as R^2, is a measure to assess the goodness of fit of the predictive model to the label data. In general, the best value for $R^2 \in [0,1]$ is 1, indicating a perfect fit. The magnitude of this value represents the quality of the fit. If the result is negative, it suggests that the model's ability to explain the data is worse than simply taking the average of the data. In such cases, the fit is considered extremely poor, and the model is not adopted. The calculation formula for R^2 is shown as Formula 08:

$$\boldsymbol{R^2 = 1 - \frac{\sum_{i=1}^{n}(y_i - \hat{y}_i)^2}{\sum_{i=1}^{n}(y_i - \bar{y})^2}} \qquad \textbf{\textit{Formula} 08}$$

Where, R^2 is coefficient of determination;

$\boldsymbol{n}$ is the number of data points;

$\boldsymbol{\bar{y}}$ is the mean value of the actual data;

$\boldsymbol{y_i}$ is the actual value of the ith data point;

$\boldsymbol{\hat{y}_i}$ is the predicted value of the ith data point.

2.4.4 Machine learning algorithm for regression

Traditionally, linear regression model has been used for relatively simple regression problems. However, when facing more complex scenarios involving multi-variables and nonlinear regression fitting, linear models may not be able to maintain good performance. Over the years, an innovative and evolving form of models has emerged, typically categorized into three phases:

Phase one: McCulloch-Pitts Model

By simplifying the structure of biological neurons, the model represented dendrites and axons as independent and dependent variables in a mathematical function, consequently allowing for simulating multivariate linear regression problems [40].

Phase two: Rosenblatt Perceptron

By introducing error and learning rate, the perceptron gained the ability to adjust its weight parameters autonomously; this capability enabled it to automatically solve linear regression problems, marking the first algorithmically complete description of a neuron. And the Learning Rate (expressed as α) is an essential adjustment parameter used in model training [41].

Phase three: BackPropagation Neural Network

By integrating backpropagation algorithm, the chain rule (extended as shown in Formula 09), and activation functions [42]. These parameters can then be adjusted using the gradient descent algorithm (as shown in Formula 10). This enables the ANN to solve extremely complex problems. Numerous scholars have explored the versatility of this model, demonstrating its compatibility with regression [43] and classification [44], while ensuring a high level of accuracy.

$$\frac{dx}{dy} = \frac{dx}{d\tau} \cdot \frac{d\tau}{d\theta} \cdot \frac{d\theta}{dy} \qquad \textit{Formula}\ \mathbf{09}$$

Where, $\frac{dx}{dy}$ ***represents the derivative of parameter*** x ***with respect to*** y***;***

$\frac{dx}{d\tau}$ ***represents the derivative of parameter*** x ***with respect to*** τ***;***

$\frac{d\tau}{d\theta}$ ***represents the derivative of parameter*** τ ***with respect to*** θ***;***

$\frac{d\theta}{dy}$ ***represents the derivative of parameter*** θ ***with respect to*** y***.***

$$x_t = x_{t-1} - \eta_t \cdot g_t \qquad \textit{Formula}\ \mathbf{10}$$

Where, x ***represents the target weight of the model parameter;***

***t* represents the current update iteration;**

***η* represents the learning rate;**

***g* represents the gradient vector of the weight parameters.**

The Neural Network algorithm has demonstrated excellent performance. Therefore, in this study, we employed the Artificial Neural Network (ANN) to conduct a regression analysis and fitting of the CEF for the FCT process.

Compared to empirical regression methods, such as Multiple Linear Regression (MLR) and logistic regression, ANN excels at handling complex nonlinear numerical fitting problems, especially when dealing with multi-parameter inputs [42]. When applied to the same dataset, ANN (R^2=0.9658) outperforms empirical multiple linear regression (R^2=0.6772) by achieving a 42.62% optimization [45]. In more complex situations, ANN can adapt by adjusting the configuration of its hidden layers, such as increasing the number of hidden layers and neurons within each layer. ANN can also be recognized as Deep Learning, when the number of hidden layers reaches 4. Research by some scholars has shown that ANN can improve the fitting ability of the model, resulting in the significant improvement of R^2 (Table 1). However, it should be pointed out that although ANN excels in regression fitting, it is susceptible to overfitting. Therefore, it is advisable to create an independent testing group validate the performance of the model.

Table 1 Comparison of fitting ability between MLR and ANN

References	Year	Empirical Algorithm	ML Algorithm	Fitting capability uprising
Leiphart & Hart [46]	2001	MLR R^2=0.74	ANN R^2=0.82	10.81%
Almetwally et al. [47]	2014	MLR R^2=0.7619	ANN R^2=0.9896	29.89%
Tiryaki & Aydın [48]	2014	MLR R^2=0.830	ANN R^2=0.997	20.12%
Ebrahimi et al. [49]	2019	MLR R^2=0.58	ANN R^2=0.64	10.34%
Hosseinzadeh et al. [50]	2020	MLR R^2=0.7290	ANN R^2=0.9991	37.05%
huang et al. [45]	2021	MLR R^2=0.6772	ANN R^2=0.9658	42.62%
Williams & Ojuri [51]	2021	MLR R^2=0.404	ANN R^2=0.955	40.20%
Chu et al. [52]	2022	MLR R^2=0.659	ANN R^2=0.939	42.49%

2.4.5 Computing platform

In this study, the mainstream machine learning algorithm, ANN, is employed for regression analysis and fitting. The model training, parameter tuning, and evaluation are conducted using the Keras library (version 2.8.0) in Python (version 3.8). Additionally, various powerful external libraries available in Python are utilized for data processing and interaction. The Pandas library (version 1.4.1) is utilized for data import and preprocessing tasks, while the Numpy library (version 1.22.3) is used for matrix computations. Visualizations and graphical representations are created using the Matplotlib library (version 3.5.1) and Seaborn library (version 0.11.2).

In terms of hardware, the CPU used is Intel i7-7700K with a clock speed of 4.20GHz. The memory capacity is Corsair 16G with a frequency of 2400MHz. The GPU employed is NVIDIA GeForce GTX 1070. For GPU hardware acceleration, the Compute Unified Device Architecture (CUDA) version used is 11.5, and the NVIDIA CUDA® Deep Neural Network Library (cuDNN) version is 8.3.1.

2.5 Experiment description

This study aims to investigate the actual operational conditions of Fossil Vehicle (FV) and Battery Electric Vehicle (BEV) under real-world road traffic scenarios, with a focus on quantifying the carbon emissions associated with component transportation. The actual carbon footprint generated during the transportation process is estimated by examining the consumption levels of fossil fuels and electricity. The study was conducted in Nanjing City of Jiangsu Province, China, and carbon dioxide emissions were calculated based on energy consumption data. To gather relevant data, the On-Board Diagnostics (OBD) interface was utilized to collect status data from the transport vehicles. Additionally, the specific test parameters, including the weight of the transported goods as indicated in the transport manifest, are outlined in Table 2.

Table 2 Variables recorded of real-world performance

Variable names	Unit for FV	Unit for BEV	Data Sources
Average speed	km/h	km/h	OBD
Energy consumption	kWh/100km	L/100km	OBD
Temperature	℃	℃	OBD
Cargo load	kg	kg	Cargo list

The experiments were conducted in Nanjing, Jiangsu Province, China. Real-world performance tests were conducted using BEV and FV. The test vehicles were in a good overall condition, with the front tire pressure of both BEVs and FVs set at 17.0±0.2 kPa, and the rear tire pressure set at 21.0±0.2 kPa. Regarding energy supply, the BEVs were charged using a 220V AC charging station with a rated power of 7 kW provided by the national power grid. The power was supplied to the BEVs' power battery pack. As for the FVs, they were fueled with 92 octane non-ethanol gasoline obtained from Sinopec gas stations. All test vehicles had a vehicle age of less than 8 years and accumulated mileage of less than 200,000 kilometers. For specific parameters, please refer to Table 3.

Table 3 Technical parameters of test vehicle

	FV [53]	BEV [54]
Type	CA1030P40Q02LE6A84	BYD5040XXYBEV3
Brand	Faw Jiefang Group Co., Ltd	BYD Auto Co., Ltd
Physical dimension	5995×2220×2380 mm	5995×2130×3150 mm
Cargo dimensions	4200×2100 mm	4030×2050 mm

Energy type	Gasoline	Electric
Energy vessel	70 Liter tank	84.4 kWh Lithium Iron Phosphate
Total quality	4490 kg	4495 kg
Curb quality	2370 kg	2450 kg
Maximum load	1995 kg	2045 kg

2.6 Function units

In this study, the total carbon emissions during the PCT process refer to the cumulative carbon emissions resulting from the energy consumed during the transportation of all prefabricated components included in a single building, from the factory to the construction site. For FV, the energy source is diesel or gasoline, while for BEV, it is the stored electrical energy in the battery pack. There can be significant differences in CE, since the transportation distances and the quantities of components vary among different projects and buildings. Therefore, in analyzing PCT data, CE per unit weight of prefabricated components per unit distance is used as an evaluation metric to mitigate the substantial impact of building scale and transportation distance on CE.

The objective of this study is to examine the Functional Unit of Carbon Emission Factor (CEF) during the PCT process. The CEF is defined as the equivalent mass of carbon dioxide emissions per kilometer traveled by one metric ton of prefabricated components, measured in kilograms of CO_2 equivalent per ton-kilometer (kg-CO_2e/(t·km)).

In this study, FV were powered by 92# gasoline, which has a density ranging from 720 to 775 kg/m^3 at a temperature of 20°C [55]. To simplify the calculation, an approximate value of 750 kg/m^3, representing the midpoint, was utilized. The carbon dioxide emission factor for gasoline is estimated to be 2.9251 kg-CO^2e/kg, resulting in a F_f value of 2.1938 kg-CO_2e/L.

The electricity consumption of BEV in China varies across different regions, primarily due to variations in the proportion of renewable energy generation in each province. In the specific experimental site of this study located in Jiangsu Province, part of the East China region, the CEF for electricity (F_e) is determined using the guidelines provided in the *Calculation standard for carbon emission from buildings (GB/T 51366-2019)* [56]. According to this standard, the F_e in this region is estimated to be 0.7035 kg-CO_2e/kWh.

3. Results

In this study, measured data were analyzed to identify the independent variables that have a significant impact on the dependent variable, the Carbon Transport Factor (CTF). These influential parameters were then used as inputs and outputs to establish a fully connected multi-layer ANN for supervised training. The study carefully selected a subset of readily available parameters as predictors of CTF, and the model demonstrated excellent fitting performance. Moreover, it was capable of simultaneously accommodating the estimation of carbon emission factors for both FV and BEV.

3.1 Preliminary data observations

This study involved a total of 658 observed data points, encompassing 5 variables. Among these variables, 4 are continuous variables. One of the variables, TOV (Type of Vehicle), is a binary variable used to distinguish between BEVs and FVs. Specifically, there are 182 data points for BEVs and 476 data points for FVs. The specific details of the variables and observations, after organizing them, are presented in Table 4.

Table 4 Statistical list of variables and observations

Variable name	Storage type	Units	Represented	Minimum observation	Maximum observation
AS	float	km	Average speed	4.33	115.50
LR	float	%	Rate of cargo weight to maximum capacity	50.00	107.04
T	float	℃	Atmosphere temperature	-17.50	36.00
TOV	boolean	-	Type of vehicle	False	True
CTF	float	kg-$CO_2e/(t\cdot km)$	Carbon emissions factor of component transportation	0.0927	1.1576

The specific distributions of the continuous variables AS, LR, T, and CTF are depicted in Figure 2. Among them, AS, T, and CTF exhibit relatively pronounced normal distributions, as indicated by their skewness and kurtosis values of [<0.0001, <0.0001], [0.0336, 0.0001], and [<0.0001, <0.0001], respectively. However, the LR parameter, due to the fixed combinations of components during transportation, primarily concentrates its data within specific intervals with the skewness and kurtosis values of [<0.0001, 0.3587]. For CTF as the dependent variable of primary interest in this study, we performed regression fitting using AS, LR, T, and TOV as independent variables, considering the distribution characteristics of the data.

Considering the capabilities of ANN in regression fitting, we directly included the binary variable TOV as one of the independent variables in the fitting analysis, eliminating the need to partition the data into different computational models based on the different categories of TOV. We employed this approach, also because in ordinary linear regression, treating a binary variable like TOV as a binary variable is necessary, but its fitting performance is often inferior to that achieved by separate regression fits for each category.

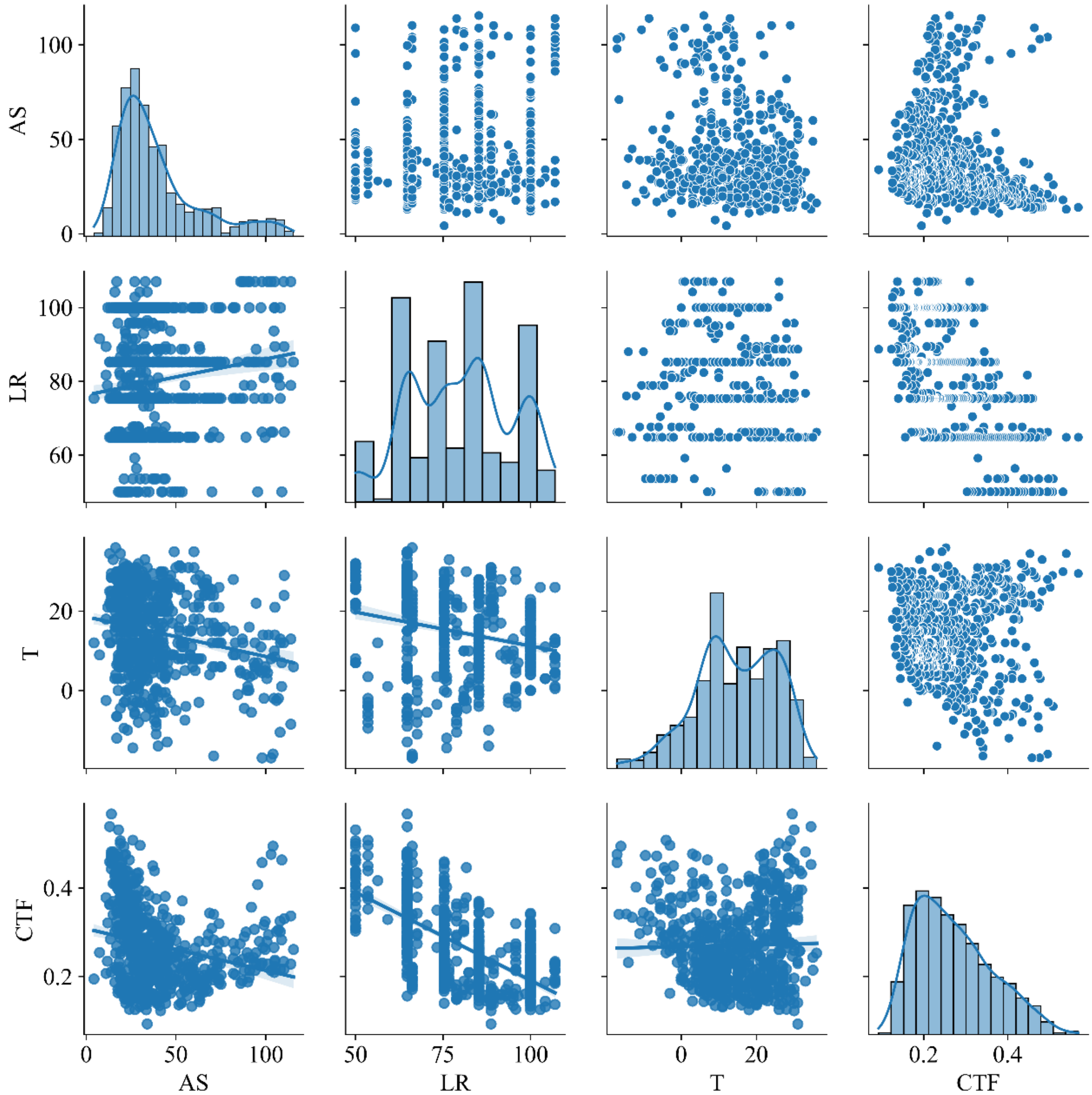

Figure 2 Distribution of continuous variable

3.2 Correlation matrix of variables

The correlation between the independent variables AS, LR, T, and TOV, and the dependent variable CTF is shown in Figure 03, with p-values less than 0.01 for all correlations. Specifically, the independent variables LR and TOV exhibit strong correlations with CTF, with correlation coefficients of -0.6130 and 0.5714, respectively, surpassing an absolute value of 0.5. The independent variable AS shows a moderate correlation with CTF, with a correlation coefficient of -0.2502, exceeding an absolute value of 0.2. On the other hand, the independent variable T demonstrates a weak correlation with CTF, with a correlation coefficient of -0.0081, below an absolute value of 0.1.

After considering the correlations between the four independent variables and the dependent variable, we retained the variables AS, LR, and TOV for subsequent machine learning training. Since obtaining the parameter of atmospheric temperature before the occurrence of component transportation (such as during the component design and lifting organization stages) is challenging and its impact on the target factor is relatively small, we excluded the variable T to eliminate the influence of atmosphere temperature on the carbon emissions factor of component transportation.

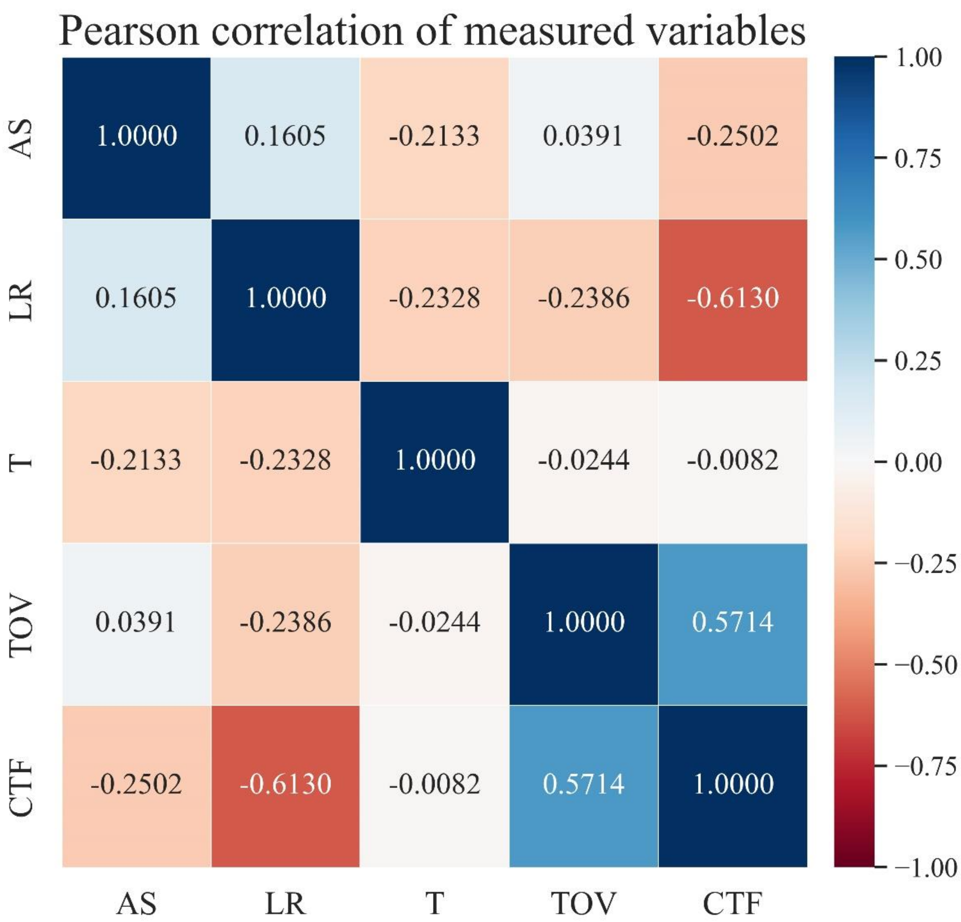

Figure 3 Pearson correlation of measured variables

3.3 Analysis between variables

The independent variables AS, LR, and TOV are moderately correlated with each other. The correlation coefficients between AS and LR, AS and TOV are 0.1605 and 0.0391, respectively, while the correlation coefficient between LR and TOV is -0.2386 (as shown in Figure 3). To further investigate their relationships, we examined the correlations among these variables and their associations with the dependent variable CTF separately.

3.3.1 Type of vehicle

As shown in Figure 4, in the PCT process, the carbon emissions of BEVs powered by electricity as fuel are not higher than those of FVs at any average velocity range or load rate range. In fact, the CE difference between BEVs and FVs tends to increase significantly, particularly at lower speeds and lower load rates. For instance, in the AS range [0-20 km/h] and the LR range [60-70%], the CE is only about 50% of that of FVs. Furthermore, this difference gradually decreases as the values of LR and AS variables increase, approaching zero when the load rate is between 90-110% and the average velocity is between 100-120 km/h.

Hence, it can be preliminarily concluded that the type of vehicle significantly affects the CTF value, and the extent of its impact follows a consistent trend in the direction of LR and AS values.

3.3.2 Average speed

As depicted in Figure 5, the relationship between CTF and AS exhibits a parabolic pattern, which is observed for both BEVs and FVs across all LR ranges. FVs demonstrate their lowest values within the range of approximately 60-70 km/h, while BEVs exhibit their lowest values within the range of approximately 40-50 km/h.

The parabolic shape of FVs is relatively steep, indicating that the CTF values vary more drastically with changes in AS. Additionally, there is a clear stratification observed across different LR ranges, where higher load rates generally correspond to lower CTF values. In other words, as the load rate increases, the CTF values tend to decrease consistently.

The parabolic shape of BEVs is relatively gentle, indicating that the changes in AS have a smaller impact on the variation of CTF values. There is a certain degree of stratification observed across different LR ranges for BEVs (although not as pronounced as in the case of FVs, which could be attributed to the comparatively smaller dataset for BEVs). Generally, a higher load rate corresponds to a lower CTF value for BEVs, following a similar trend as observed for FVs.

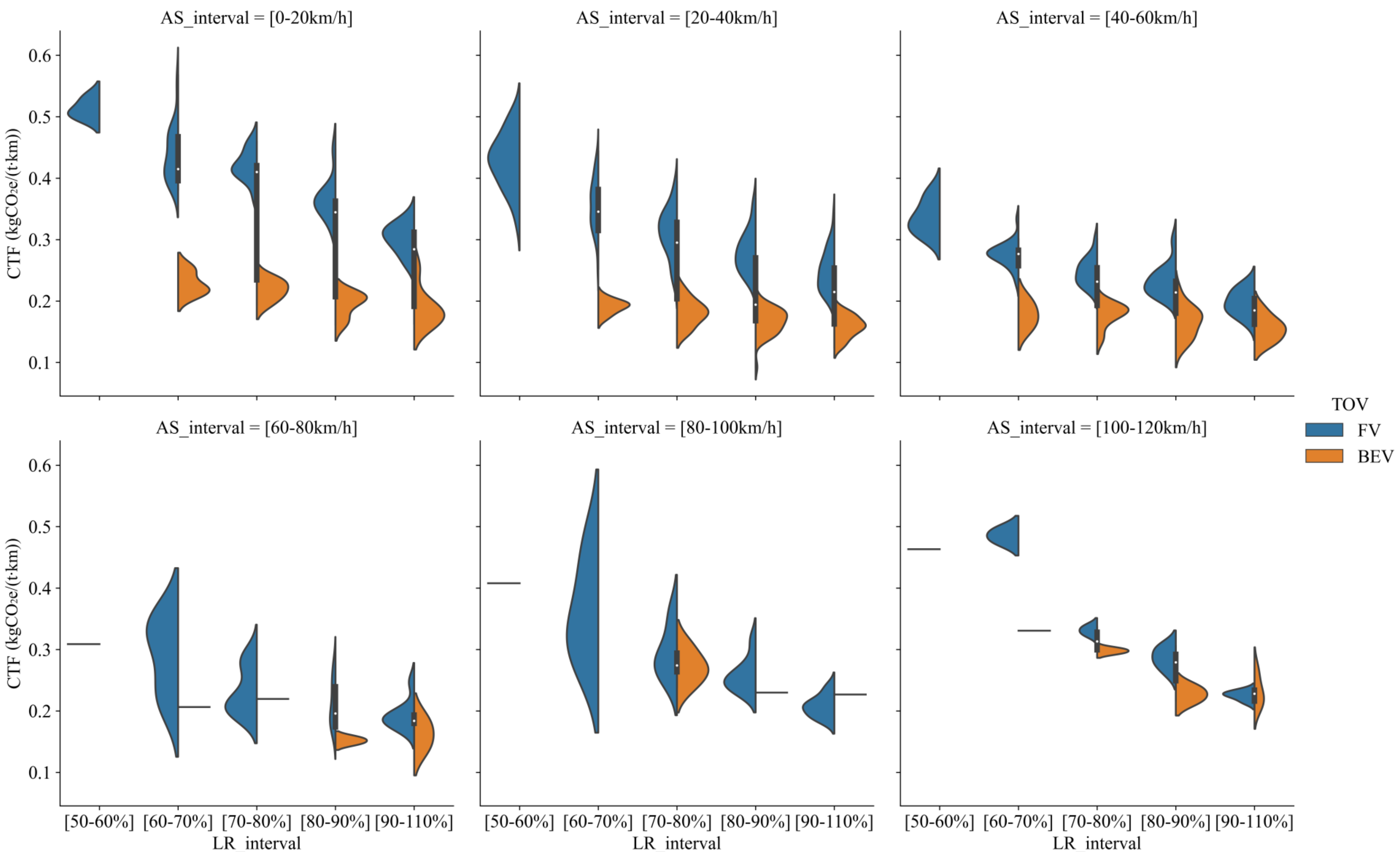

Figure 4 Violin plot for contrasting FV and BEV at different AS & LR interval

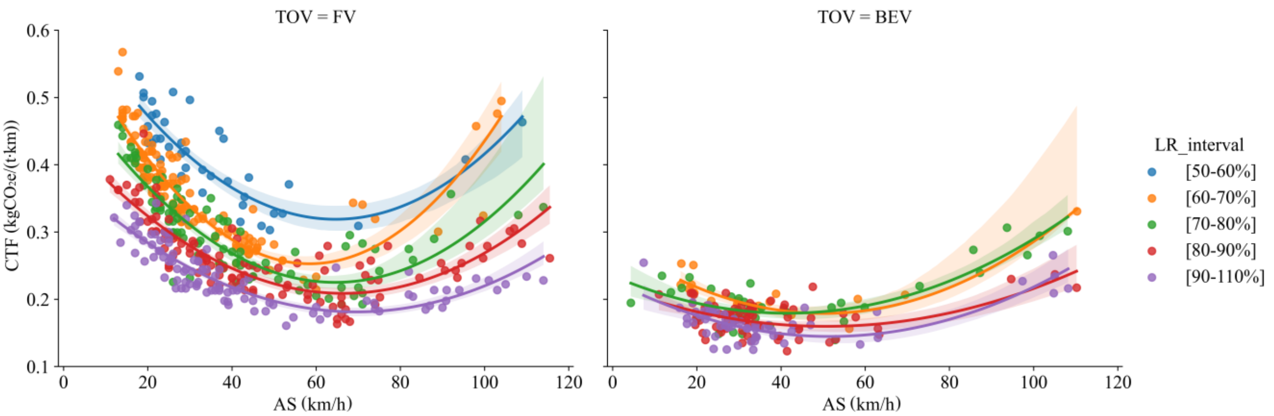

Figure 5 Relationship between CTF and AS at different LR interval

3.3.3 Load rate

Figure 6 shows an inverse relationship between CTF and LR, indicating that the CTF values decrease as the LR values increase. And this trend is observed for both BEVs and FVs across all LR ranges.

Within the FV group, the CTF exhibits a significant range of variation. There is a distinct stratification observed across different AS ranges, where the CTF values are lowest in the 60-80 km/h range and progressively increase in adjacent order.

Within the BEV group, the CTF exhibits a relatively gentle range of variation. Similarly, there is a noticeable stratification observed across different AS ranges, where the CTF values are lowest in the 40-60 km/h range and progressively increase in adjacent order.

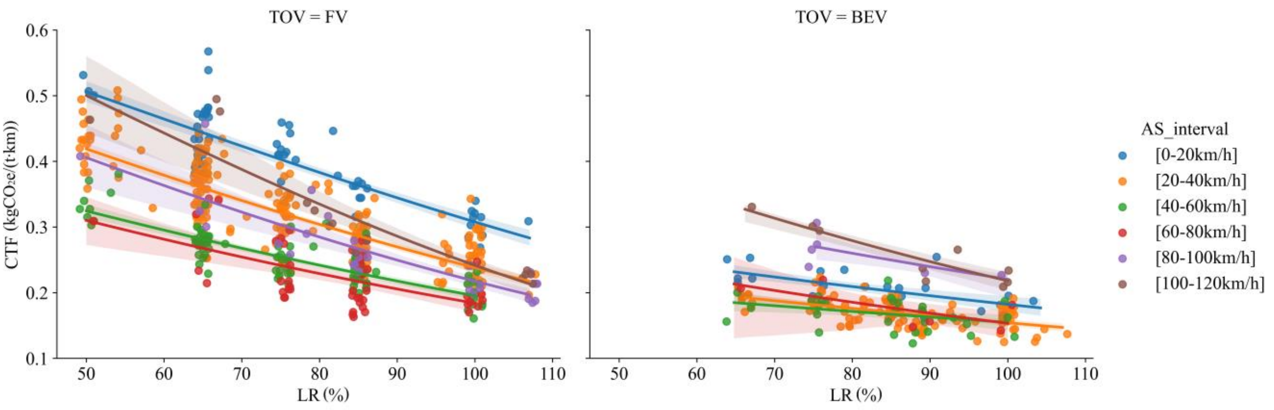

Figure 6 Relationship between CTF and LR at different AS interval

3.4 Training of Artificial Neural network

Due to the powerful regression fitting capabilities of ANN, this study employed a Cross Validation approach to divide the data into training group and testing group, with the value of K-fold set to 5. The random variable value for each iteration was set to a fixed value, which ensured that the two groups of data were consistently fixed, enabling a convenient comparison of the model's effectiveness.

3.4.1 Fundamental setting

Given the training data size is approximately 1K, Stochastic Gradient Descent (SGD) was employed to optimize computational resource utilization.

Since this study focuses on regression rather than classification tasks, the commonly used Mean Squared Error (MSE) was chosen as the loss function. As for the learning rate, it was initially set to 0.1.

In the initial phase, an ANN configuration with two hidden layers, each containing 5 neurons, was utilized. The performance of four widely used activation functions—Sigmoid, Tanh, ReLU, and Leaky ReLU—was extensively compared. After careful evaluation, Sigmoid was determined to be the most suitable choice as the final activation function.

In order to prevent overfitting, the initial training phase did not incorporate Dropout to reduce excessive reliance on specific neurons within the network. If the training results are unsatisfactory, the possibility of introducing Dropout with a value of 0.5 or 0.8 could be considered. Additionally, the regularization technique can be adjusted from L1 to L2. In the subsequent computational process, the model achieved the predetermined objective, with a Dropout value of 1.0 and regularization set to L1.

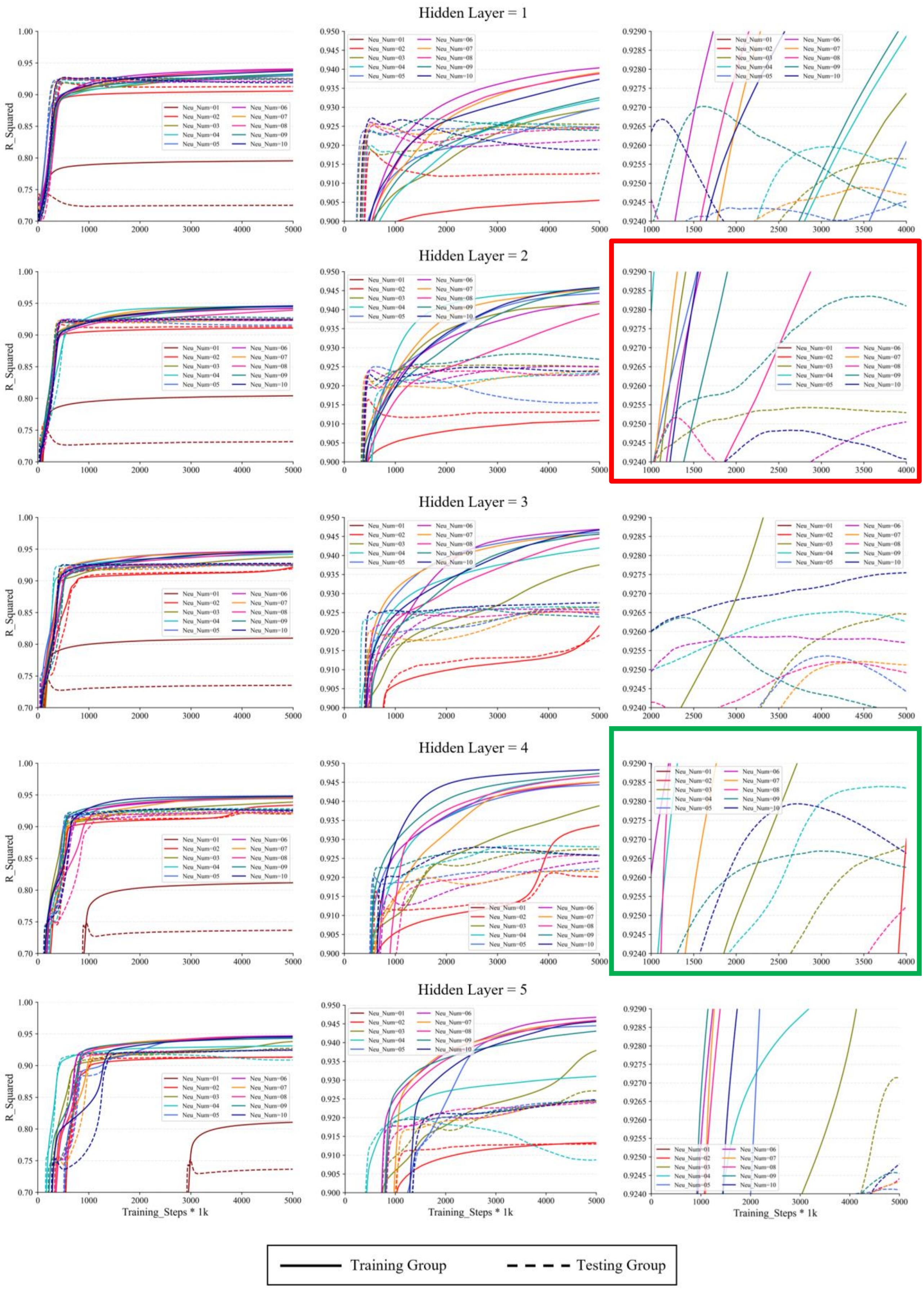

Figure 7 Relationship between R^2 and Training step at different hidden layer and neural number

3.4.2 Structure selection of network

Figure 7 shows the training results for a fixed training step of 5 million obtained by traversing the number of hidden layers from 1 to 5 and the number of neurons per layer from 1 to 10. It is important to note that increasing the number of hidden layers and neurons does not necessarily lead to better training results. In fact, excessively complex model structures can often result in the occurrence of gradient vanishing during the training process. Therefore, obtaining an appropriate ANN configuration becomes crucial in achieving desirable outcomes.

For the configuration with 2 hidden layers and 9 neurons per layer, the testing group achieved an R^2 value of 0.92835. The optimal solution was obtained when the training step reached 3,576,000. In this "9-9" configuration, the total number of neurons in the hidden layers is 18, as indicated by the red outlined section in Figure 7.

For the configuration with 4 hidden layers and 4 neurons per layer, the testing group achieved an R^2 value of 0.92839. The optimal solution was obtained when the training step reached 3,680,000. In this "4-4-4-4" configuration, the total number of neurons in the hidden layers is 16, as indicated by the green outlined section in Figure 7.

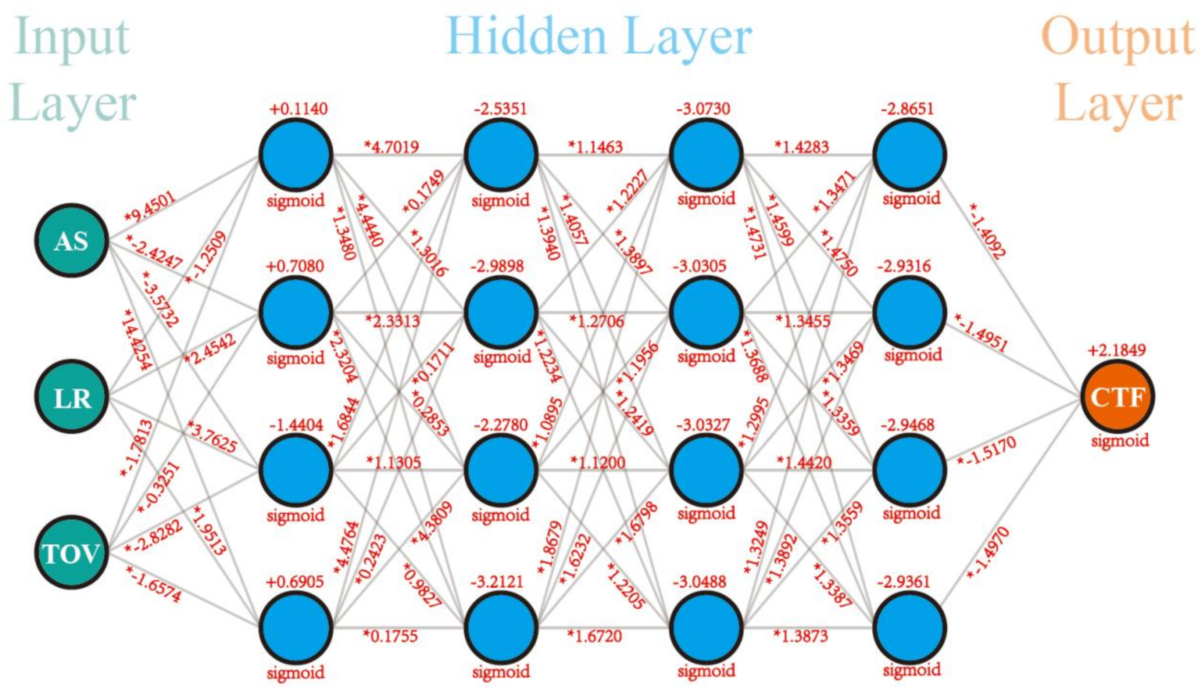

Figure 8 Adopted ANN framework and parameters of calculating model for CTF

Considering both the R^2 value and model complexity, the "4-4-4-4" configuration is chosen as the final architecture. The final ANN computational model framework and parameters are illustrated in Figure 8.

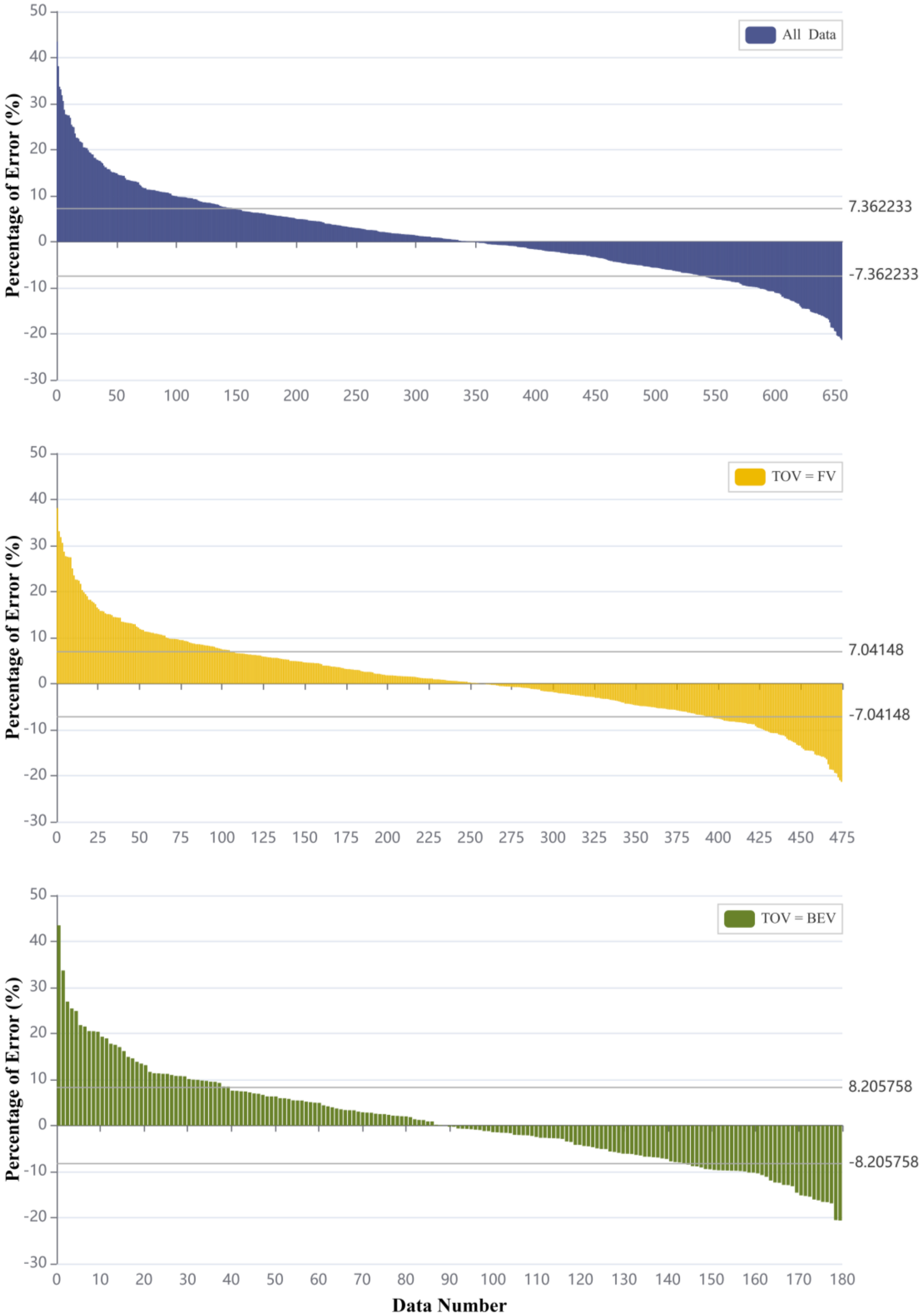

Figure 9 Error of model fitting for adopted ANN structure

3.5 Accuracy for predicting CTF

In the context of CTF value prediction（Figure 9), we examined three scenarios: the overall situation, FV, and BEV. These scenarios were evaluated based on their predictive accuracy compared to the available data, as depicted in Figure 9. The Mean Absolute Percentage Error (MAPE) for the overall scenario was calculated to be 7.4486%. Similarly, the FV scenario yielded a MAPE of 7.0415%, while the BEV scenario demonstrated a slightly higher MAPE of 8.5133%. Notably, the accuracy of FCT prediction surpassed 90%.

In our study, we employed different models to address the regression problem. The "3-4-4-4-4-1" Artificial Neural Network (ANN) configuration, after training, achieved an impressive R^2 value of 0.92839. In contrast, the Multiple Linear Regression model yielded a comparatively lower R^2 value of 0.6035, indicating a significant 53.83% improvement in model fitting performance when using the ANN model. These findings align with previous studies conducted by various researchers [48-55]. It is evident that the ANN model exhibits a substantial advantage in accurately fitting regression data. However, it is important to note that training the ANN model was a time-intensive process, taking a total of 20,843 seconds, which is approximately equivalent to 5.79 hours.

Table 5 CTF at different average speed and load rate

Average Speed	**Load Rate**					
	50%	**60%**	**70%**	**80%**	**90%**	**100%**
20km/h	0.479453/ **0.251846** (-47.47%)	0.424303/ **0.221648** (-47.76%)	0.378086/ **0.200020** (-47.10%)	0.339790/ **0.184410** (-45.73%)	0.308270/ **0.172987** (-43.88%)	0.282414/ **0.164488** (-41.76%)
40km/h	0.334341/ **0.238844** (-28.56%)	0.298664/ **0.209052** (-30.00%)	0.269594/ **0.187753** (-30.36%)	0.245945/ **0.172509** (-29.86%)	0.226696/ **0.161490** (-28.76%)	0.211001/ **0.153405** (-27.30%)
60km/h	0.304342/ **0.261444** (-14.10%)	0.272001/ **0.224379** (-17.51%)	0.245856/ **0.197509** (-19.66%)	0.224723/ **0.178283** (-20.67%)	0.207605/ **0.164523** (-20.75%)	0.193694/ **0.154580** (-20.19%)
80km/h	0.319232/ **0.313225** (-1.88%)	0.283195/ **0.263248** (-7.04%)	0.254058/ **0.225469** (-11.25%)	0.230572/ **0.197903** (-14.17%)	0.211620/ **0.178124** (-15.83%)	0.196276/ **0.163968** (-16.46%)

CTF for FVs/**BEVs** (percentage reduction)
Units: kg-CO_2e/(t·km)

3.6 Comparison of BEV and FV

Due to the distinctive nature of PCB, the selection of transportation schemes for the PCT process prioritized the timely delivery of prefabricated components with the required specifications to the construction site. In this context, transportation efficiency became of lesser importance than this primary objective. Factors such as maximizing space utilization during component loading and minimizing congestion during transportation became secondary considerations. As a result, the transportation of components, in comparison to material transportation, exhibits lower efficiency, characterized by reduced load rates and average speeds.

BEVs have demonstrated remarkable adaptability to the specific characteristics of the PCT process. Table 5 presents the practical measurements of BEVs during component transportation, considering various load rates and average speeds, alongside the corresponding FV scenarios. The table reveals noteworthy insights: lower load rates correspond to higher carbon reduction proportions for BEVs compared to FVs. Moreover, although BEVs consistently exhibit lower carbon emissions across different average speeds, the relationship between load rates and carbon reduction proportions exhibits distinct patterns within each speed range.

For example, at a load rate of 50% and an average speed of 20 km/h, the CTF value stands at 0.251846 kg-CO_2e/(t·km), resulting in a significant 47.47% reduction in carbon emissions compared to the FV scenario. Conversely, when operating at a load rate of 100% and an average speed of 60 km/h, the CTF value decreases to 0.154580 kg-CO_2e/(t·km), translating to a commendable 20.19% reduction in carbon emissions compared to the FV scenario. Notably, the former exhibits an impressive increase of 27.28 percentage points in carbon reduction compared to the latter.

However, in previous comparative case studies, although PCB was established as a lower-carbon option, it showed higher carbon emissions during the transportation stage. This is primarily due to the inclusion of an additional secondary transportation link in PCT, which is less efficient compared to material transportation. If BEV is used to replace FV for both component and material transportation, the low-carbon potential of PCB is expected to be further explored.

4. Discussion

In this study, we developed the calculating model, which effectively captured the carbon emission characteristics of component transportation under real-world conditions through the fitting of CTF using ANN. The model exhibited high accuracy and can reflect the carbon emissions of both FV and BEV under different scenarios, while also demonstrating the influence of external parameters and providing quantitative data support for making macro-level PCT decisions.

4.1 Influence mechanism of LR and AS on CTF

During the transportation of components, a vehicle's total weight comprises its own weight (unladen weight) and the payload it carries, which contribute equally to fuel consumption. Consequently, a smaller LR results in a higher proportion of fuel consumption. Thus, when transporting components of equal weight over the same distance, more fuel is wasted on the vehicle's unladen weight, leading to increased carbon emissions and a higher CTF value (Figure 6). In extreme scenarios, such as when LR is extremely low or even approaches zero, the carbon emissions caused by the vehicle's own weight remain a factor. During these circumstances, if the payload PCs are used and the CEs corresponding to each ton of PCs are calculated, the CTF tends to approach infinity. That mechanism applies to both BEVs and FVs. This conclusion is consistent with the previous results of various researchers. In cases involving vehicle transport for passages, where the self-weight to load weight ratio is higher, the energy consumption only increases by 9% ~ 11%when comparing full load to no-load conditions [30].

During vehicle operations, various resistances must be overcome, taking into account factors such as gear ratios. As a result, there exists an optimal range for fuel efficiency during vehicle operation. Excessive average speeds, on the other hand, lead to a rapid increase in aerodynamic drag, rolling resistance, and internal mechanical resistance, ultimately resulting in higher CTF values. Typically, the optimal fuel efficiency range for a FV is around 80 km/h , while for BEVs, which lack a transmission mechanism, the optimal range is approximately 60 km/h (Figure 5).

In urban areas, where PCBs are usually situated, the speed limits typically range from 50 to 60 km/h. In these speed ranges, BEVs tend to operate more efficiently compared to FVs. Also, urban areas tend to have denser traffic with more frequent traffic lights, increasing the chances of encountering red lights, which results in longer idle times. For BEVs, the engine remains in a standby state in the idle times and consumes almost no energy. However, due to the nature of internal combustion engines, FVs need to maintain energy consumption levels even when idling. Therefore, in the 0-60 km/h speed range, the lower the average speed, the greater the BEVs' contribution to emission reduction.

Indeed, excessively low average speeds can also lead to higher CTF values. This is because, during urban driving conditions, a significant portion of the vehicle's idle time is spent waiting at traffic lights. This idle time contributes to increased fuel consumption while the vehicle remains stationary. In the context of the PCT process, a decrease in the average speed (AS) often signifies more idle time and frequent start-stop situations. Consequently, at a macro level, this reduces fuel efficiency and results in higher carbon emissions.

It is worth noting that BEVs exhibit significantly lower energy consumption during idle states compared to FVs that rely on internal combustion engines to remain operational. That is consistent with the conclusions of previous studies [24, 25]. As a result, BEVs are less affected by changes in AS, leading to a lower sensitivity of CTF with respect to AS variations.

4.2 Potential for applying BEV in PCT

The characteristics of BEV, namely their ability to achieve higher decarbonization efficiency under low load rate and low average speed conditions compared to FV (Table 5), make them a promising option during the widespread adoption of PCB, as the direct carbon emissions during the PCT process can be effectively reduced to zero by using BEVs (Figure 4).

Taking the year 2022 in Nanjing City as an example, there were 1,218 newly constructed prefabricated buildings involving a total of 1,044,590 prefabricated components. The estimated total weight of these components amounts to approximately 1 million metric tons (calculated based on an average weight of 1 ton per component). Assuming a transportation distance of 50 kilometers within the city, if all the component transportation is carried out using BEVs with an average speed of 40 km/h and a load rate of 60%, it would result in a carbon reduction of 4,680 metric tons, equivalent to a reduction rate of 30.00% compared to FV scenarios. This conclusion is consistent with the results of other studies focusing on passenger transportation by private cars [31], taxis [33], and buses [32].

4.3 Contribution

This study makes a significant contribution by adopting a more objective approach to obtaining carbon emission factors, particularly in contrast to the prevailing methods used in China for deriving transportation-related carbon emission factors. Currently, carbon emissions during the transportation of components are estimated solely based on the carbon emission factors provided in *Calculation standard for carbon emission from buildings* [56]. However, these factors only provide a rough outline and are applicable solely to the transportation of basic construction materials at half load rate, taking into account return factors. When applying 2 ton level vehicle for transportation, the carbon emission factor for gasoline is 0.334 kg-CO_2e/(t·km) and for diesel it is 0.286 kg-CO_2e/(t·km). Simply applying these carbon emission factors to estimate the Carbon Transport Factor (CTF) in the PCT process would only consider the vehicle-level emissions and overlook the variations in carbon emissions among different prefabricated component transportation schemes. The limitation hinders the optimization and control of carbon emissions. In contrast, the calculating model developed in this research can accurately reflect the actual driving conditions and loading status, before the transportation occurs. This means that optimization efforts to reduce carbon emissions can be achieved based on the model's calculation.

Furthermore, it is important to note that the mentioned standard [56] does not provide any guidance algorithms for cases involving electric transportation. This study has made a noteworthy contribution in addressing the aforementioned issues. When considering an average speed of 40 km/h and 50% load rate, the carbon emission factors for gasoline vehicles provided in Table 5 are basically consistent with the aforementioned standards. However, the carbon emission factor for BEV is merely 0.239 kg-CO2e/(t·km). This means that for regular material transportation, if a BEV is used, the above-mentioned coefficients can be directly used. The low-carbon benefits and advantages of BEVs in component transportation have not only been acknowledged in raw material transportation [57], but also in public transportation [32], and even private transportation [31, 33]. Research has demonstrated that by substituting BEVs for FVs in non-long-distance transportation, carbon emissions can be significantly reduced.

To encourage the adoption of new transportation methods involving BEVs, authorities can use administrative levers to promote a low-carbon industry. For example, contractors who use BEVs in component transportation can receive corresponding carbon trading points or even tax exemptions. In innovative implementation of such policies can not only benefit the building sector, but also contribute to carbon reduction in the road transportation sector, which accounts for 8.8% of global carbon emissions [58].

It is important to focus on optimizing carbon emissions during the design phase of PCBs. Many factors influence the carbon emission during the materialization phase, such as constraints on the stacking layers, transportation height, and transportation width. Additionally, the size of components must strike a balance between the lifting capacity of cranes and the efficiency of hoisting. To solve and analyze optimization problems at each stage, advanced algorithms such as Genetic Algorithms and Generative Adversarial Networks are crucial. These algorithms are especially essential for production, transportation, and installation.

4.4 Future works

It is essential to acknowledge that the computational model was trained using vehicles weighing around 2 tons. Therefore, we cannot guarantee its applicability to larger and medium-sized transport vehicles. To ensure that the research outcomes can be adapted to a broader range of scenarios, it is recommended that subsequent research focuses on conducting a comparative study between BEVs and FVs for medium and large-sized vehicles, with a significant sample size of carbon emission measurements. Additionally, introducing the vehicle class as an additional input parameter in the computational model is crucial. By incorporating data from medium and large-sized vehicles and considering different vehicle classes, the modified computational model will offer enhanced accuracy and applicability for a wider range of transport scenarios.

The Neural Network-based model used in this study demonstrates commendable performance in regression fitting. However, it is essential to address the considerable training time, which can take nearly 6 hours per iteration. In this study, since we needed to explore and compare various configurations such as different hidden layer structures, activation functions, and learning rates, the cumulative training time exceeded 10 days. Such lengthy training time severely limited the practical applicability of obtaining reasonable CEF. Given the current limitations in achieving significant hardware breakthroughs within a short time frame, it is recommended to explore alternative algorithms, such as Gradient Boosting Decision Tree, Random Forest, and eXtreme Gradient Boosting, to improve training efficiency.

5. Conclusions

Compared with the cast-on-site construction method, the additional CEs generated during PCT process must be lower than the reduced CEs during the construction and production stage, in order to ensure the total embodied carbon reduction of PCB. This study explored the carbon reduction potential and its constraints of using BEVs in the PCT process by collecting real road control data, fitting analysis, and establishing a carbon emission factor calculation model. The main findings are as follows:

(1) In this study, we utilized ANN through supervised learning with real-world data to develop a fitting calculation model for estimating carbon emissions during the PCT process -with a high R^2 of 0.9284 and MAPE of 7.4486%-is versatile enough to accommodate both fossil and electric vehicles. Although the focus is on China, by calibrating fossil fuel and electricity carbon emission factors across regions, the research is applicable to other countries for estimating CE in PCT.

(2) Employing BEVs can achieve carbon reduction compared to FVs in any PCT case, and the maximum reduction can reach an impressive 47.76%. Additionally, the research revealed a positive correlation between lower average speeds and lower load rates with higher carbon reduction percentages for BEVs, that's what often happens in prefabricated components transportation. The popularity of BEVs in the context of PCT is expected to increase significantly.

(3) Emphasizing the significant potential of BEVs in achieving emission reductions. The research filled the gap of factor missing of Adopting BEV in transportation especially for prefabricated components. Participants in PCB can use the calculation model to optimize the architecture design, prefabricated component arrangement and transportation schedule for better CE reduction.

Acknowledge:

This work was supported by National Key Research and Development Program of China [Grand No. 2022YFC3803804], National Natural Science Foundation of China [Grand No. 51978137 and 51908111], Nanjing Construction Industry Modernization Research Project [Grand No. 2021003], and SRTP project of Southeast University [Grand No. 202310286006Z]

Reference

[1] Tu, R., Li, T., Meng, C., Chen, J., Sheng, Z., Xie, Y., ... & Liu, Y. (2021). Real-world emissions of construction mobile machines and comparison to a non-road emission model. Science of The Total Environment, 771, 145365. https://doi.org/10.1016/j.scitotenv.2021.145365.

[2] Qi, Y., Stern, N., He, J. K., Lu, J. Q., Liu, T. L., King, D., & Wu, T. (2020). The policy-driven peak and reduction of China's carbon emissions. Advances in Climate Change Research, 11(2), 65-71. https://DOI10.1016/j.accre.2020.05.008.

[3] Zhang, Y., Hu, S., Guo, F., Mastrucci, A., Zhang, S., Yang, Z., & Yan, D. (2022). Assessing the potential of decarbonizing China's building construction by 2060 and synergy with industry sector. Journal of Cleaner Production, 359, 132086. https://doi.org/10.1016/j.jclepro.2022.132086

[4] Shi, Q., Chen, J., & Shen, L. (2017). Driving factors of the changes in the carbon emissions in the Chinese construction industry. Journal of Cleaner Production, 166, 615-627. https:// DOI10.1016/j.jclepro.2017.08.056.

[5] Akbarnezhad, A., & Xiao, J. (2017). Estimation and minimization of embodied carbon of buildings: A review. Buildings, 7(1), 5. https://doi.org/10.3390/buildings7010005.

[6] Hu, S., Zhang, Y., Yang, Z., Yan, D., & Jiang, Y. (2022, November). Challenges and opportunities for carbon neutrality in China's building sector—Modelling and data. In Building Simulation (Vol. 15, No. 11, pp. 1899-1921). Beijing: Tsinghua University Press.

[7] Dixit, M. K. (2019). Life cycle recurrent embodied energy calculation of buildings: A review. Journal of cleaner production, 209, 731-754. https://doi.org/10.1016/j.jclepro.2018.10.230.

[8] Qian, Y., Leng, J., Chun, Q., Wang, H., & Zhou, K. (2023). A year-long field investigation on the spatio-temporal variations of occupant's thermal comfort in Chinese traditional courtyard dwellings. Building and Environment, 228, 109836. https://doi.org/10.1016/j.buildenv.2022.109836

[9] Thiel, C. L., Campion, N., Landis, A. E., Jones, A. K., Schaefer, L. A., & Bilec, M. M. (2013). A materials life cycle assessment of a net-zero energy building. Energies, 6(2), 1125-1141. https://DOI10.3390/en6021125.

[10] Zhang, X., Shen, L., & Zhang, L. (2013). Life cycle assessment of the air emissions during building construction process: A case study in Hong Kong. Renewable and Sustainable Energy Reviews, 17, 160-169. https://DOI10.1016/j.rser.2012.09.024.

[11] Dimoudi, A., & Tompa, C. (2008). Energy and environmental indicators related to construction of office buildings. Resources, Conservation and Recycling, 53(1-2), 86-95. https://DOI10.1016/j.resconrec.2008.09.008.

[12] Peng, C. (2016). Calculation of a building's life cycle carbon emissions based on Ecotect and building information modeling. Journal of Cleaner Production, 112, 453-465. https://DOI10.1016/j.jclepro.2015.08.078.

[13] Zhang, Y., Yan, D., Hu, S., & Guo, S. (2019). Modelling of energy consumption and carbon emission from the building construction sector in China, a process-based LCA approach. Energy Policy, 134, 110949. https://doi.org/10.1016/j.enpol.2019.110949

[14] Koukkari, H., & Sarvakanta, L. (2005). Ageing challenges in the construction sector. International Journal of Strategic Property Management, 9(2), 91-97. https://DOI10.1080/1648715X.2005.9637530.

[15] Hong, J., Shen, G. Q., Li, Z., Zhang, B., & Zhang, W. (2018). Barriers to promoting prefabricated construction in China: A cost–benefit analysis. Journal of cleaner production, 172, 649-660. https://DOI10.1016/j.jclepro.2017.10.171.

[16] Ng, J. Y., & Chan, A. H. (2018). The work ability of Hong Kong construction workers in relation to individual and work-related factors. International Journal of Environmental Research and Public Health, 15(5), 990. https://DOI10.3390/ijerph15050990.

[17] Zhang, X., Skitmore, M., & Peng, Y. (2014). Exploring the challenges to industrialized residential building in China. Habitat International, 41, 176-184. https://DOI10.1016/j.habitatint.2013.08.005.

[18] Cao, X., Li, X., Zhu, Y., & Zhang, Z. (2015). A comparative study of environmental performance between prefabricated and traditional residential buildings in China. Journal of cleaner production, 109, 131-143. https://DOI10.1016/j.jclepro.2015.04.120.

[19] J.L. Hao, B. Cheng, W. Lu, J. Xu, J. Wang, W. Bu, Z. Guo, Carbon emission reduction in prefabrication construction during materialization stage: A BIM based life-cycle assessment approach, Sci. Total Environ. 723 (2020), https:// doi.org/10.1016/j.scitotenv.2020.137870.

[20] Wong, F., & Tang, Y. T. (2012). Comparative embodied carbon analysis of the prefabrication elements compared with in-situ elements in residential building development of Hong Kong. International Journal of Civil and Environmental Engineering, 6(2), 89-94.

[21] Dong, Y. H., Jaillon, L., Chu, P., & Poon, C. S. (2015). Comparing carbon emissions of precast and cast-in-situ construction methods–A case study of high-rise private building. Construction and building materials, 99, 39-53. https:// DOI10.1016/j.conbuildmat.2015.08.145

[22] Mao, C., Shen, Q., Shen, L., & Tang, L. (2013). Comparative study of greenhouse gas emissions between off-site prefabrication and conventional construction methods: Two case studies of residential projects. Energy and Buildings, 66, 165-176. https://DOI10.1016/j.enbuild.2013.07.033.

[23] Xiang, Y., Ma, K., Mahamadu, A. M., Florez-Perez, L., Zhu, K., & Wu, Y. (2023). Embodied carbon determination in the transportation stage of prefabricated constructions: A micro-level model using the bin-packing algorithm and modal analysis model. Energy and Buildings, 279,

112640. https://doi.org/10.1016/j.enbuild.2022.112640.

[24] Ding, Z., Liu, S., Luo, L., & Liao, L. (2020). A building information modeling-based carbon emission measurement system for prefabricated residential buildings during the materialization phase. Journal of Cleaner Production, 264, 121728. https://doi.org/10.1016/j.jclepro.2020.121728

[25] Wang, H., Zhang, H., Hou, K., & Yao, G. (2021). Carbon emissions factor evaluation for assembled building during prefabricated component transportation phase. Energy Exploration & Exploitation, 39(1), 385-408. https://DOI10.1177/0144598720973371.

[26] Dubois, A., & Gadde, L. E. (2002). The construction industry as a loosely coupled system: implications for productivity and innovation. Construction https://doi.org/10.1080/01446190210163543management & economics, 20(7), 621-631.

[27] U.S.E.P.A. EPA, Exhaust Emission Rates for Light-Duty Onroad Vehicles in MOVES3, 2020.

[28] Lu, T., Yao, E., Jin, F., & Pan, L. (2020). Alternative incentive policies against purchase subsidy decrease for battery electric vehicle (BEV) adoption. Energies, 13(7), 1645. https://DOI10.3390/en13071645.

[29] Yu, A., Wei, Y., Chen, W., Peng, N., & Peng, L. (2018). Life cycle environmental impacts and carbon emissions: A case study of electric and gasoline vehicles in China. Transportation Research Part D: Transport and Environment, 65, 409-420. https://DOI10.1016/j.trd.2018.09.009.

[30] Zhou, B., Wu, Y., Zhou, B., Wang, R., Ke, W., Zhang, S., & Hao, J. (2016). Real-world performance of battery electric buses and their life-cycle benefits with respect to energy consumption and carbon dioxide emissions. Energy, 96, 603-613. https://DOI10.1016/j.energy.2015.12.041.

[31] von Brockdorff, P., & Tanti, G. (2017). Carbon emissions of plug-in electric vehicles in Malta: A policy review. Case Studies on Transport Policy, 5(3), 509-517. https://DOI10.1016/j.cstp.2017.05.002.

[32] Xu, Y., Gbologah, F. E., Lee, D. Y., Liu, H., Rodgers, M. O., & Guensler, R. L. (2015). Assessment of alternative fuel and powertrain transit bus options using real-world operations data: Life-cycle fuel and emissions modeling. Applied energy, 154, 143-159. https://DOI10.1016/j.apenergy.2015.04.112.

[33] Jenn, A. (2020). Emissions benefits of electric vehicles in Uber and Lyft ride-hailing services. Nature Energy, 5(7), 520-525. https://DOI10.1038/s41560-020-0632-7.

[34] Pollet, B. G., Staffell, I., & Shang, J. L. (2012). Current status of hybrid, battery and fuel cell electric vehicles: From electrochemistry to market prospects. Electrochimica Acta, 84, 235-249. https://DOI10.1016/j.electacta.2012.03.172.

[35] Correa, G., Muñoz, P., Falaguerra, T., & Rodriguez, C. R. (2017). Performance comparison of

conventional, hybrid, hydrogen and electric urban buses using well to wheel analysis. Energy, 141, 537-549. https://DOI10.1016/j.energy.2017.09.066.

[36] Zolghadr, A., Gharaie, E., & Naderpajouh, N. (2022). Barriers to innovation in the housing sector: Economic justifiability of offsite construction for housebuilders. Journal of Building Engineering, 52, 104490. https://DOI10.1016/j.jobe.2022.104490.

[37] Lee, D. Y., Thomas, V. M., & Brown, M. A. (2013). Electric urban delivery trucks: Energy use, greenhouse gas emissions, and cost-effectiveness. Environmental science & technology, 47(14), 8022-8030. https://DOI10.1021/es400179w.

[38] Wang, H., Zhang, H., Zhao, L., Luo, Z., Hou, K., Du, X., ... & Lu, Y. (2022). Real-world carbon emissions evaluation for prefabricated component transportation by battery electric vehicles. Energy Reports, 8, 8186-8199. https://DOI10.1016/j.egyr.2022.06.039.

[39] Protocol, K. (1997). Kyoto protocol. UNFCCC Website. Available online: http://unfccc. int/kyoto_protocol/items/2830. php (accessed on 1 January 2011).

[40] McCulloch, W. S., & Pitts, W. (1943). A logical calculus of the ideas immanent in nervous activity. The bulletin of mathematical biophysics, 5, 115-133. https://DOI10.1016/S0092-8240(05)80006-0.

[41] Rosenblatt, F. (1958). The perceptron: a probabilistic model for information storage and organization in the brain. Psychological review, 65(6), 386. https://DOI10.1037/h0042519.

[42] Rumelhart, D. E., Hinton, G. E., & Williams, R. J. (1986). Learning representations by back-propagating errors. nature, 323(6088), 533-536. https://DOI10.1038/323533a0.

[43] Momeni, E., Nazir, R., Armaghani, D. J., & Maizir, H. (2014). Prediction of pile bearing capacity using a hybrid genetic algorithm-based ANN. Measurement, 57, 122-131. https://DOI10.1016/j.measurement.2014.08.007.

[44] LeCun, Y., Bengio, Y., & Hinton, G. (2015). Deep learning. Nature, 521(7553), 436-444. https://DOI10.1038/nature14539.

[45] Huang, X., Wang, H., Luo, W., Xue, S., Hayat, F., & Gao, Z. (2021). Prediction of loquat soluble solids and titratable acid content using fruit mineral elements by artificial neural network and multiple linear regression. Scientia Horticulturae, 278, 109873. https://doi.org/10.1016/j.scienta.2020.109873

[46] Leiphart, D. J., & Hart, B. S. (2001). Case history: Comparison of linear regression and a probabilistic neural network to predict porosity from 3-D seismic attributes in Lower Brushy Canyon channeled sandstones, southeast New Mexico. Geophysics, 66(5), 1349-1358. https://doi.org/10.1190/1.1487080

[47] Almetwally, A. A., Idrees, H. M., & Hebeish, A. A. (2014). Predicting the tensile properties of cotton/spandex core-spun yarns using artificial neural network and linear regression models. The Journal of the Textile Institute, 105(11), 1221-1229.

https://doi.org/10.1080/00405000.2014.882043

[48] Tiryaki, S., & Aydın, A. (2014). An artificial neural network model for predicting compression strength of heat treated woods and comparison with a multiple linear regression model. Construction and Building Materials, 62, 102-108. https://doi.org/10.1016/j.conbuildmat.2014.03.041

[49] Ebrahimi, M., Sarikhani, M. R., Sinegani, A. A. S., Ahmadi, A., & Keesstra, S. (2019). Estimating the soil respiration under different land uses using artificial neural network and linear regression models. Catena, 174, 371-382. https://doi.org/10.1016/j.catena.2018.11.035

[50] Hosseinzadeh, A., Baziar, M., Alidadi, H., Zhou, J. L., Altaee, A., Najafpoor, A. A., & Jafarpour, S. (2020). Application of artificial neural network and multiple linear regression in modeling nutrient recovery in vermicompost under different conditions. Bioresource technology, 303, 122926. https://doi.org/10.1016/j.biortech.2020.122926

[51] Williams, C. G., & Ojuri, O. O. (2021). Predictive modelling of soils' hydraulic conductivity using artificial neural network and multiple linear regression. SN Applied Sciences, 3, 1-13.

[52] Chu, C., Boré, A., Liu, X. W., Cui, J. C., Wang, P., Liu, X., ... & Bary, A. (2022). Modeling the impact of some independent parameters on the syngas characteristics during plasma gasification of municipal solid waste using artificial neural network and stepwise linear regression methods. Renewable and Sustainable Energy Reviews, 157, 112052. https://doi.org/10.1016/j.rser.2021.112052

[53] https://product.360che.com/s31/7791_64_param.html

[54] https://cv.byd.com/cv/carShow.html-param=T5

[55] Yang, J., Ma, Y., Fu, J., Shu, J., & Liu, J. (2019). Parametric study of gasoline properties on combustion characteristics of gasoline compression engines using reaction kinetics simulation and density-based global sensitivity analysis. Applied Energy, 255, 113858. https://DOI10.1016/j.apenergy.2019.113858

[56] Standardization Administration of the People's Republic of China. GB/T 51366-2019 Calculation standard for carbon emission from buildings, 2019.

[57] Gao, Z., Lin, Z., & Franzese, O. (2017). Energy consumption and cost savings of truck electrification for heavy-duty vehicle applications. Transportation Research Record, 2628(1), 99-109. https://doi.org/10.3141/2628-11

[58] https:// Teter, J., Cazzola, P., Gul, T., Mulholland, E., Le Feuvre, P., Bennett, S., ... & Maroney, E. (2017). The future of trucks: Implications for energy and the environment (pp. 1-167). International Energy Agency, IEA..org/10.1088/2634-4505/ac6442